CHEMISTRY
A EUROPEAN JOURNAL

DOI: 10.1002/chem.200500933

Versatile Coordination Chemistry towards Multifunctional Carbon Nanotube Nanohybrids

Dirk M. Guldi,*[a] G. M. Aminur Rahman,[a] Shuhui Qin,[b] Maxim Tchoul,[b] Warren T. Ford,[b] Massimo Marcaccio,[c] Demis Paolucci,[c] Francesco Paolucci,[c] Stéphane Campidelli,[d] and Maurizio Prato[d]

Dedicated to Professor Fred Wudl on the occasion of his 65th birthday

Abstract: Dispersible single-walled carbon nanotubes grafted with poly(4-vinylpyridine), SWNT-PVP, were tested in coordination assays with zinc tetraphenylporphyrin (ZnP). Kinetic and spectroscopic evidence corroborates the successful formation of a SWNT-PVP·ZnP nanohybrid. Within this SWNT-PVP·ZnP nanohybrid, static electron-transfer quenching $(2.0\pm0.1)\times10^{9}\,s^{-1}$ converts the photoexcited-ZnP chromophore into a radical-ion-pair state with a microsecond lifetime, namely one-electron oxidized-ZnP and reduced-SWNT.

Keywords: charge transfer · donor–acceptor systems · nanotubes · porphyrinoids · radical ions

Introduction

Nanometer-scale structures are under intense investigation with aim of producing innovative materials, composites, and electronic devices of greatly reduced size.[1] Among the wide range of available structures, carbon nanostructures provide a good example of great potential in materials science. Carbon nanotubes (CNT), and in particular, single-walled carbon nanotubes (SWNT) are graphene cylinders with diameters typically on the nanometer scale.[2–4] These cylinders have typical lengths of micrometers, with a unique blend of mechanical, electrical, thermal, and optical properties.[5–7] Consequently, the development of methodologies for integrating CNT into functional structures, such as ultralight composites, and donor–acceptor hybrids, has emerged as an area of intense research.[8–11]

However, processing and applications of CNT have been hindered by difficulty in manipulation, mainly due to the high intertube attraction energies. The most common way to produce clean, individual CNT involves extensive horn sonication and/or the use of strongly oxidizing agents (such as nitric acid, sulfuric acid, hydrogen peroxide, ozone oxidation, and so on).[12] But such drastic conditions bring about major changes in the π-electronic structure and, subsequently, in the properties of CNT.[13–15] Moreover, CNT degradation will inevitably take place.

To improve CNT solubility, while decreasing CNT aggregation, two general strategies have been devised. First, the sp^2-hybridized structure of graphene can be covalently functionalized by using groups that increase the interaction with the surrounding medium.[4] Second, noncovalent functionalization through π–π interactions allows the formation of stable suspensions, while leaving the graphene structure intact.[16–17]

Once functionalized, CNT can be employed in a variety of innovative fields. Among these, CNT find use as acceptors in donor–acceptor hybrid materials for applications in solar energy conversion.[8,17,18] Work performed either in condensed media or at electrode surfaces demonstrated that the presence of extended, delocalized π-electron systems is, indeed, very useful for inducing charge transfer and charge transport. For example, illumination of CNT-based donor–

[a] Prof. D. M. Guldi, Dr. G. M. A. Rahman
Friederich-Alexander-University Erlangen-Nürnberg Institute for Physical Chemistry
Egerlandstrasse 3, 91058 Erlangen (Germany)
Fax: (+49) 9131-852-8307
E-mail: dirk.guldi@chemie.uni-erlangen.de

[b] Dr. S. Qin, M. Tchoul, Prof. W. T. Ford
Department of Chemistry, Oklahoma State University
Stillwater, OK 74078 (USA)

[c] Dr. M. Marcaccio, Dr. D. Paolucci, Prof. F. Paolucci
Dipartimento di Chimica "G. Ciamician"
University of Bologna
Via Selmi, 2, 40126 Bologna (Italy)

[d] Dr. S. Campidelli, Prof. M. Prato
Dipartimento di Scienze Farmaceutiche
University of Trieste
Piazzale Europa 1, 34127 Trieste (Italy)

Supporting information for this article is available on the WWW under http://www.chemeurj.org/ or from the author.

acceptor nanohybrids with visible light is typically followed by fast charge separation and slow charge recombination. The lifetimes of the charge-separated radical-ion-pair states are so long that these systems can be used for the fabrication of photovoltaic devices.[10,18]

In the present work we combine the covalent and noncovalent approaches to provide a route towards versatile donor–acceptor hybrid structures. SWNT were grafted with poly(4-vinylpyridine), PVP, to form DMF-soluble SWNT-PVP (see Scheme 1).[19] The pyridine moieties present in SWNT-PVP favor the axial coordination of a strong donor in the excited state, zinc tetraphenylporphyrin (ZnP).

Results and Discussion

The SWNT-PVP was prepared by free-radical polymerization of 4-vinylpyridine in a dispersion of pristine high-pressure carbon monoxide, (HiPCO) SWNT in DMF. Free PVP and SWNT catalyst residues were removed by a series of centrifugation and decantation steps. Thermogravimetric analysis of SWNT-PVP gave a SWNT-to-PVP weight ratio of 61/39 with less than 1% residual catalyst.[19]

Two regions of transitions are discernable in the absorption spectra. First, the UV part that corresponds to the polymer.[20] Second, the visible and near-infrared part (see Figure 1) where the characteristic van Hove singularities of SWNT (bandgap transitions in semiconducting and metallic SWNT) are typically seen. The fact that van Hove singularities are present indicates that only minor modification of the electronic structure had occurred during the free-radical polymerization. The absorption measurements were also used to estimate the SWNT-PVP concentration at 18.6 mg L^{-1}.

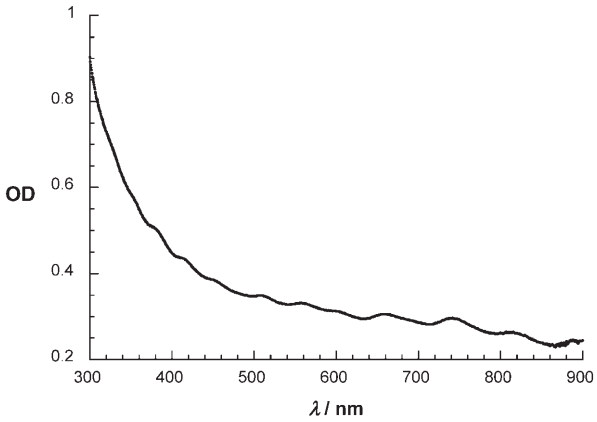

Figure 1. Room temperature absorption spectrum of SWNT-PVP in DMF.

Raman spectra of solid SWNT-PVP showed a small increase in the D-band suggesting a low degree of functionalization of the SWNT side walls and minor changes in the

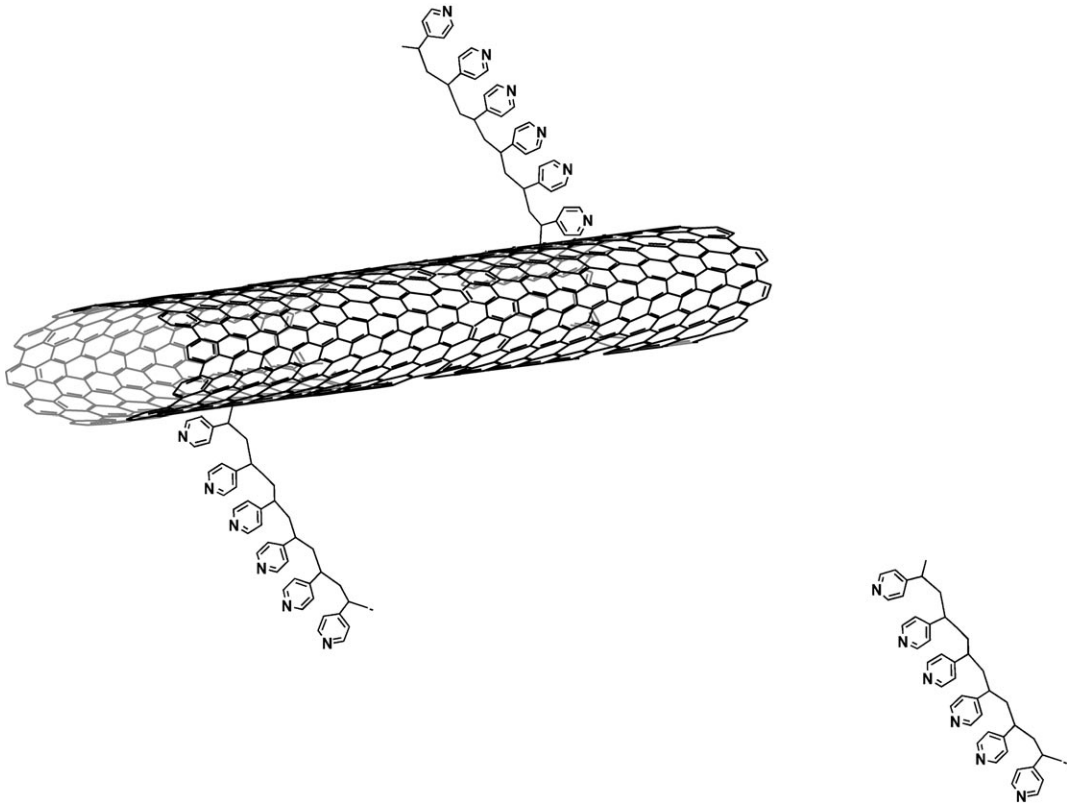

Scheme 1. Compounds used in this study: SWNT-PVP (left) and PVP (right).

radial breathing modes indicating little perturbation of the electronic structure relative to pristine SWNT.[19]

The distribution of diameters and lengths of SWNT-PVP were determined by tapping-mode AFM. From typical images, as shown in Figure 2, individual SWNT and small

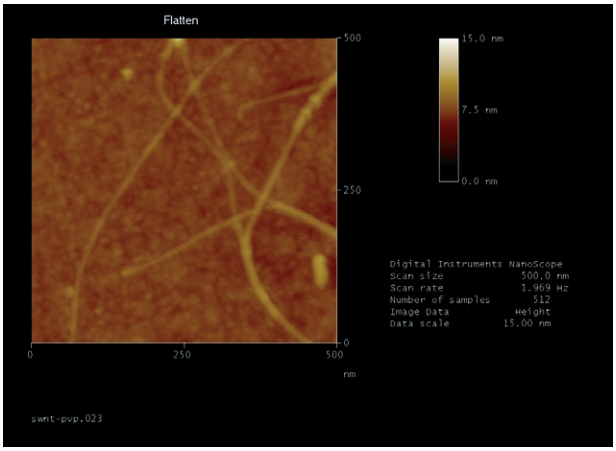

Figure 2. AFM height images of SWNT-PVP on a mica surface.

bundles are discernable, the lengths of which vary between several hundred nanometers and several micrometers. The heights of tubes, on the other hand, range from 0.8 to 3.2 nm with an average of 1.5 nm matching the diameters of individual pristine SWNT that are usually from 0.6 to 1.3 nm. Overall the presence of PVP chains leads to apparently thicker SWNT contours. Consequently, we correlate the 1.5 nm height of the SWNT-PVP with individual tubes. A qualitative similar conclusion is derived from TEM measurements. Figure 3 shows some representative TEM images of SWNT-PVP that were recorded with different magnifications.

SWNT-PVP can be fully dispersed in DMF, yielding suspensions that are stable for months. Electronic interactions between SWNT and PVP in the excited state are assumed from the fact that the PVP-centered fluorescence in SWNT-PVP is largely quenched (such as by a factor >10, see Figure S1 in the Supporting Information) relative to PVP, which was employed as a reference.

Cyclic voltammetric (CV) experiments were carried out in SWNT-PVP dispersions obtained upon short (≤ 1 min) sonication in either DMF or THF, with tetrabutylammonium hexafluorophosphate as supporting electrolyte. The CV pattern obtained in DMF was complicated by strong adsorption phenomena at ~ -0.5 and -1 V, which made the identification of the voltammetric features associated to SWNT-PVP unfeasible. THF was therefore chosen, in spite of the much lower loadings of nanotubes achieved in that solvent. The CV curve shown in Figure 4 (dashed line) displays, at potentials ≥ -2.2 V, the typical continuum of (low-intensity) diffusion-controlled cathodic current, with onset at ~ -0.5 V (Figure 4, inset), that was already observed in the case of pyrrolidine-functionalized SWNT, investigated under similar

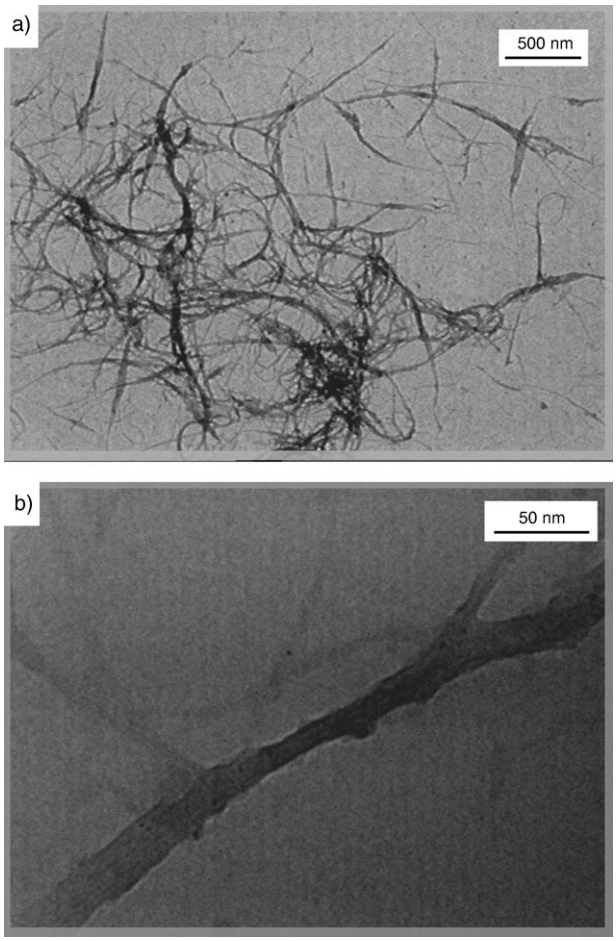

Figure 3. TEM pictures of SWNT-PVP with different magnifications: see scale bars for details.

conditions.[8c,f] Such a current is associated with the reduction of SWNT.[8f] A sharp increase of the cathodic current (I) was observed at potentials ≤ -2.5 V attributed to: 1) the increase in the electronic density of state of SWNTs,[8f] 2) the parallel reduction of the pyridyl moieties in the PVP chains. In fact, the latter process is responsible for the broad and irreversible cathodic shoulder located at about -2.6 V (and for the coupled anodic peak observed at -1.4 V in the reverse scan). Prolonged sonication (30 min) of the THF solution, along with a large increase of its optical density (OD) indicative of a larger dispersion of SWNT-PVP, brought about the significant enhancement of the above voltammetric features (Figure 4, solid line). However, the presence of a novel reduction peak located at -2.2 V, in the CV curve of the heavily sonicated solution, also suggests that some degradation of PVP-SWNT is likely to occur under such conditions.

The complexation of ZnP with SWNT-PVP, a sketch for which is shown in Scheme 2, and also with PVP was checked by spectroscopic fluorescence and absorption titration experiments. In particular, various concentrations of SWNT-PVP or PVP were added to a ZnP solution in DMF (approximately 5 μM) without affecting the overall SWNT-PVP

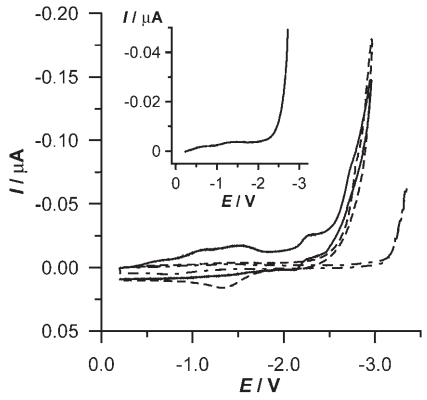

Figure 4. CV curves of a SWNT-PVP in 0.05 M TBAH/THF solution, run after prolonged (——) and short sonication (-----). The dash-dot line (–•–•) corresponds to the response of the blank supporting electrolyte solution. Inset: baseline-corrected CV curve, run after short sonication. Scan rate = 1.0 $V s^{-1}$, $T = 25\,°C$. Working electrode: Pt disc ($r = 62.5$ mm). Potentials were measured versus silver quasi-reference electrode.

concentration. The solutions of SWNT-PVP and PVP were matched at the 300 nm absorption to guarantee comparable concentrations in the two independent sets of titration experiments. With increasing SWNT-PVP concentration the ZnP absorption features (Soret and Q-band) revealed bathochromic shifts, up to around 2 nm. These shifts were further accompanied by small but notable broadenings and isosbestic points at around 422 and 429 nm. The presence of the isosbestic points implies a clean conversion from ZnP to SWNT-PVP•ZnP. Most evident are the shifts in the Soret-band region (400–450 nm), where the van Hove singularities of SWNT-PVP do not interfere to any significant extent with the porphyrin transitions (Figure 5a).[21] In contrast, in the region of the Q-bands (500–600 nm), the absorption of the SWNT prevents a meaningful spectral analysis (Figure 5b). The same bathochromic shifts in the Soret band developed when just PVP or pyridine were mixed with ZnP.

The shifts observed, though small, indicate a ligand-exchange reaction. The solvent DMF is, in fact, a coordinating agent itself, thus competing with pyridine for the complexation of the ZnP.[22] From this we conclude that the bathochromic shifts reflect electronic effects that evolve from a tighter metal-to-ligand coordination.

The fluorescence emission experiments with ZnP allow a distinction between coordinating SWNT-PVP or PVP. Figure 6 shows the steady-state fluorescence with 429 nm excitation (the isosbestic point in the absorption measurements). In particular, when adding SWNT-PVP, the ZnP fluorescence quantum yields ($\Phi = 0.04$) under aerated or deaerated conditions drop exponentially approaching asymptotically Φ base values of approximately 0.01. In line with previous findings, we assign this behavior to static elec-

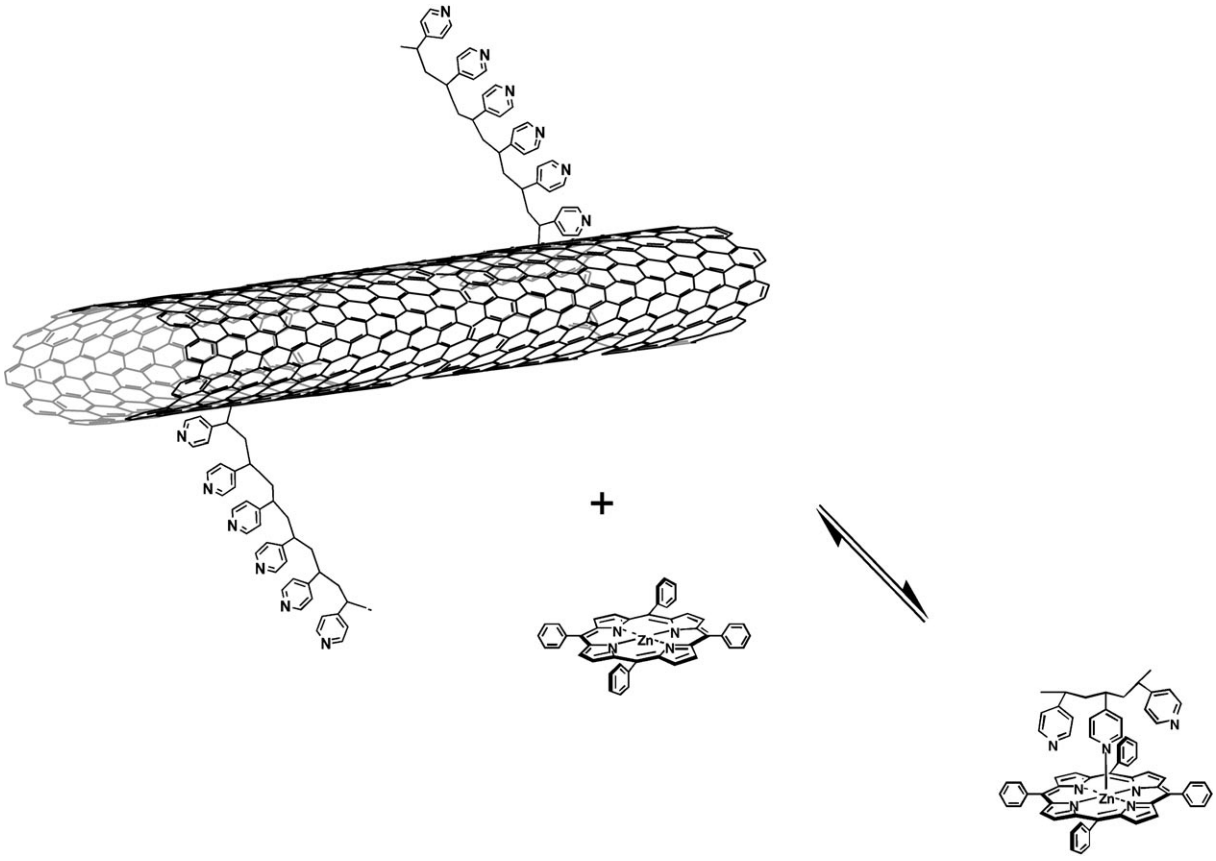

Scheme 2. Partial structure of SWNT-PVP that coordinates axially to ZnP.

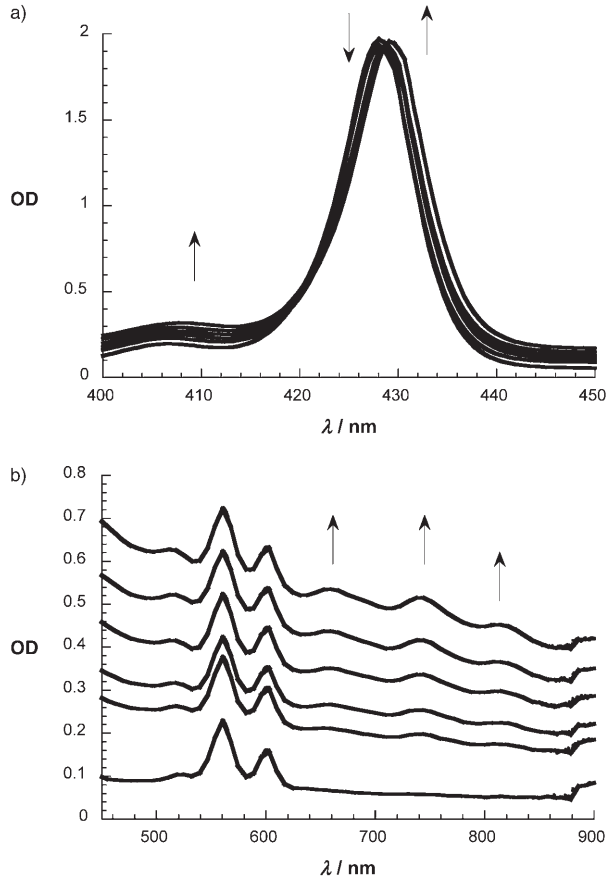

Figure 5. a) Absorption spectra of ZnP (5 μM) in DMF after addition of variable SWNT-PVP concentrations. b) Absorption spectra of ZnP (5 μM) in DMF after addition of variable SWNT-PVP concentrations.

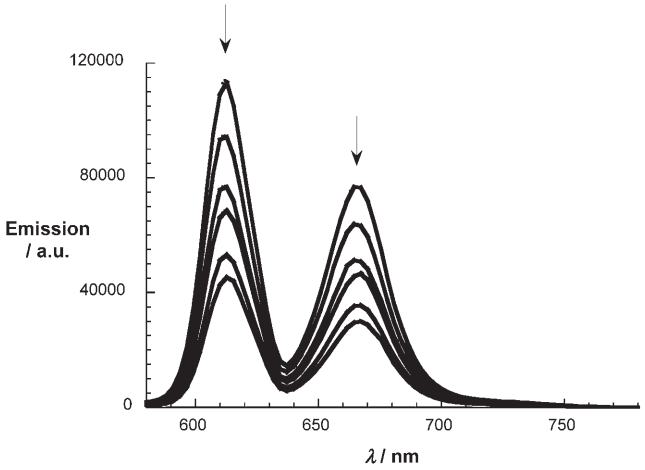

Figure 6. Fluorescence spectra of ZnP (5 μM) in DMF after addition of variable SWNT-PVP concentrations. The excitation wavelength is the isosbestic point at 429 nm.

tron-transfer quenching within a SWNT-PVP•ZnP complex (vide infra). Besides the quenching, we also observe red-shifts of the fluorescence maxima, similar to the absorption spectra. With the help of the fluorescence base-value and the fluorescence features of ZnP (fluorescence quantum yield (Φ) of 0.04 and fluorescence lifetime (τ) of 2.0 ns) we estimate the underlying intrahybrid electron-transfer rate to be $(1.8\pm0.5)\times10^9\ s^{-1}$ from Equation (1).

$$k = [\Phi_{(ZnP)} - \Phi_{(SWNT\text{-}PVP\cdot ZnP)}]/[\tau_{(ZnP)}\ \Phi_{(SWNT\text{-}PVP\cdot ZnP)}] \quad (1)$$

In sharp contrast, a reference experiment using PVP gives no appreciable fluorescence quenching (see Figure S2 in the Supporting Information). The lack of any electron-accepting character of PVP is responsible for the absence of fluorescence quenching.[23] Despite the unchanged fluorescence values, the maxima exhibit the expected red-shift. Similar findings also emerged in parallel experiments, when pyridine was added to a solution of ZnP in DMF.

A series of blank experiments with SWNT (pristine SWNT and SWNT-PVP) were also performed. In particular, SWNT-PVP was titrated with free-base tetraphenylporphyrin (H_2P, see Figure S3 and S4 in the Supporting Information). The lack of shifts in the absorption spectrum confirms the absence of coordination. However, a moderate H_2P fluorescence quenching of less than 20% was observed, which suggests some other pathways of excited-state deactivation. It should be noted that for SWNT-PVP•ZnP under comparable conditions the quenching is more than 65% (see Figure 6). To investigate the SWNT–H_2P interactions, similar concentrations of pristine SWNT, suspended in DMF, were added to H_2P and/or ZnP, giving identical results of no shift in absorption and about 20% fluorescence quenching. It is reasonable to deduce π–π interactions to be responsible for the residual fluorescence quenching.[24]

Kinetic support for an electron-transfer deactivation came from complementary time-resolved fluorescence measurements. For ZnP in aerated DMF the fluorescence decay is best fitted, with a χ^2 value of approximately one, by a monoexponential expression that yields a lifetime of 1.94 ± 0.1 ns. On the other hand, in SWNT-PVP•ZnP, the decay profile is diexponential with a long-lived (1.94 ± 0.1 ns) and a short-lived (0.41 ± 0.05 ns) component (see Figure S5, Supporting Information). Table 1 summarizes the most relevant fluorescence parameters of solutions containing different SWNT-PVP/ZnP ratios. The resemblance of the former value with that of just ZnP alone, namely, prior to the addition of

Table 1. Time-resolved fluorescence data for SWNT-PVP•ZnP.

ZnP	aliquots SWNT-PVP	fluorescence lifetime [ns][a]	fluorescence lifetime [ns][b]	fluorescence lifetime [ns][c]	ratio between lifetimes
5 μM	0	1.94			
5 μM	1	1.89	0.39		1.42
5 μM	2	2.0	0.38		1.07
5 μM	3	2.3	0.41		0.71
0	3			1.3	

[a] Long-lived component: intrinsic ZnP fluorescence deactivation. [b] Short-lived component: electron-transfer quenching. [c] PVP fluorescence lifetime.

SWNT-PVP, suggests a regular fluorescence deactivation of free ZnP. In other words, it refers to ZnP that is not coordinated to SWNT-PVP. The shorter lifetime, however, corresponds to the actual electron-transfer quenching determined by Equation (2) as $(1.9\pm0.1)\times10^{9}\ s^{-1}$, which occurs within the photoexcited SWNT-PVP•ZnP complex.

$$k = 1/\tau_{(SWNT\text{-}PVP\cdot ZnP)} - 1/\tau_{(ZnP)} \quad (2)$$

Notably, a good agreement is established between the extrapolated value and that determined in the steady-state experiments - vide supra. As the SWNT-PVP concentration is increased, the same two-component decays are noted throughout the titration experiments. Only the relative contributions change, that is, the relative weight of the short-lived component increases steadily with increasing SWNT-PVP, while that of the long-lived component decreases simultaneously (see Table 1). At the end-point of the titration, the short-lived component predominates. In line with the aforementioned observation, upon titrating ZnP with PVP or pyridine, only a monoexponential decay is seen throughout the entire series of experiments. Moreover, the decays always reflect the intrinsic ZnP fluorescence lifetime of 2.0 ± 0.2 ns. Similarly, in SWNT-PVP/H_2P and SWNT/H_2P only the long-lived component of free H_2P (9.5 ± 0.5 ns) is seen.

All these data point to a static and rapid singlet-excited-state quenching event occurring inside well-defined nanohybrids of SWNT-PVP•ZnP. The most likely excited-state quenching process involves electron transfer, namely, oxidation of the ZnP and reduction of the SWNT [Eq. (3)].

$$\text{SWNT-PVP}\cdot\text{ZnP} \xrightarrow{light} \text{SWNT-PVP}\cdot(^{1*}\text{ZnP}) \rightarrow (\text{SWNT}^{\cdot-}\text{-PVP})\cdot(\text{ZnP}^{\cdot+}) \quad (3)$$

Transient absorption measurements were performed to confirm the nature of the fluorescence quenching. The concept here is to photoexcite ZnP or SWNT-PVP•ZnP with short (6 ns) laser pulses at 532 nm, a wavelength that corresponds to the area of Q-band absorption. Following the rapid excitation, we should be able: 1) to visualize the transient and/or stable products, 2) resolve their formation/decay kinetics, and 3) to make a quantitative and qualitative comparison between the two cases.

In the case of ZnP alone, after a time delay of 50 ns we see the characteristic triplet–triplet fingerprints (Figure 7). In particular, transient bleaching of the Soret and Q-band develops, and is further accompanied by a characteristic triplet signature at 800 nm.[25] The ZnP triplet-excited state is oxygen-sensitive ($k_{oxygen}=6.5\times10^{8}\ M^{-1}\ s^{-1}$), causing the formation of singlet oxygen, and decays under oxygen-free conditions with a lifetime of typically around 50 μs under our experimental conditions.

Appreciable differences can be observed following photoexcitation of SWNT-PVP•ZnP (see Figure 8). After a time delay of 50 ns, important changes are the broad 600–800 nm absorptions and the lack of the triplet feature at 800 nm. Interestingly, the oscillator strength of the new transient, although the ZnP concentration in SWNT-PVP•ZnP is identical to that used for the ZnP reference experiment, is stronger.[26] The new features, especially the 600–800 nm absorption, are those of the one-electron-oxidized ZnP product,

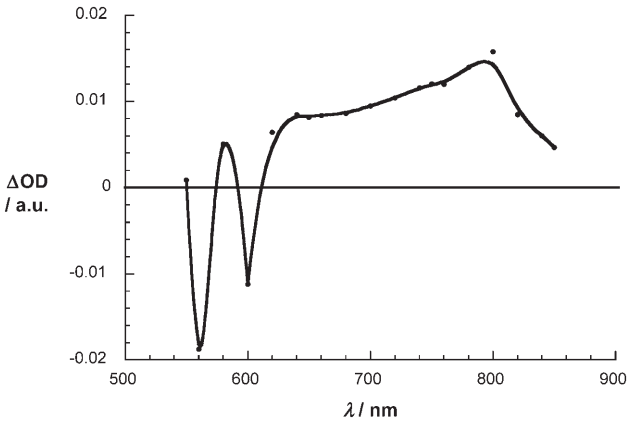

Figure 7. Nanosecond transient absorption spectrum following the 532 nm excitation of ZnP in DMF (time delay is 50 ns) shown are the triplet–triplet features of ZnP.

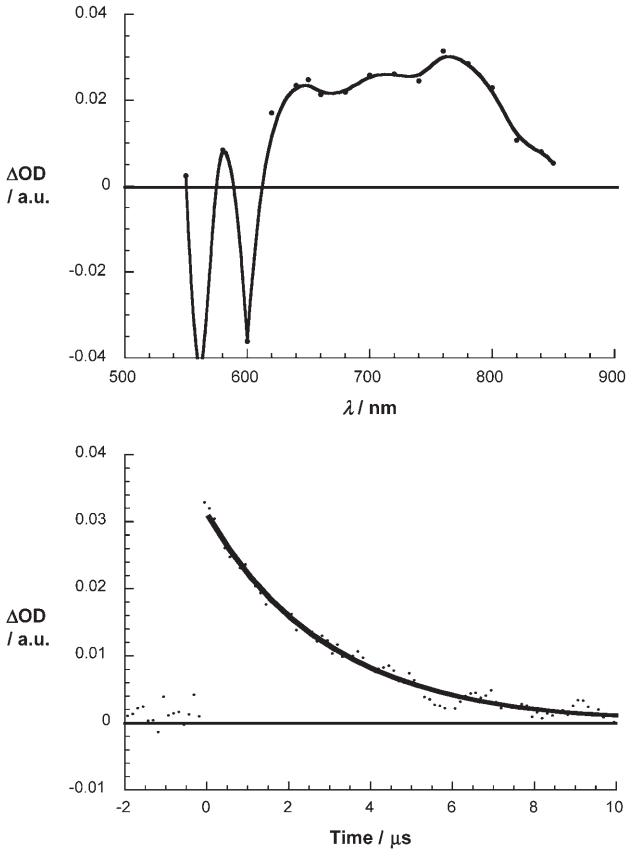

Figure 8. Top: Nanosecond transient absorption spectrum following the 532 nm excitation of SWNT-PVP•ZnP in DMF (time delay is 50 ns) shown are the ZnP radical cation features. Bottom: Time-absorption profiles at 760 nm.

namely, the π-radical cation. The transient absorption spectrum obtained upon one-electron pulse-radiolytic oxidation of ZnP in oxygenated dichloromethane containing 1 vol% pyridine is displayed in Figure 9.[27] From the type of features we postulate that an intracomplex electron transfer, evolving from the photoexcited ZnP to the electron-accepting SWNT-PVP, governs the photoexcited-state deactivation of SWNT-PVP•ZnP.

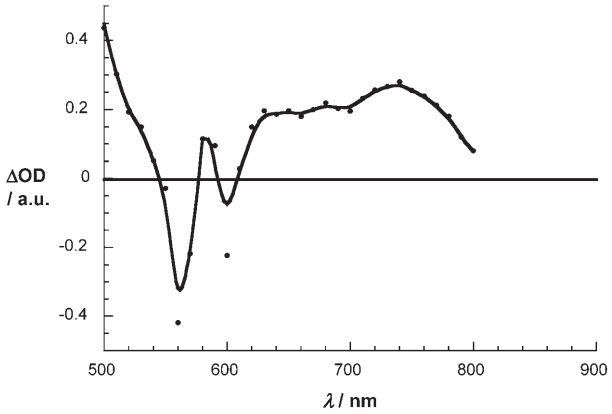

Figure 9. Differential absorption spectrum (UV/Vis spectrum) monitored 200 μs after pulse radiolytic oxidation of ZnP in oxygenated dichloromethane solutions containing 1 vol% pyridine.

Analysis of the time–absorption profiles gave a respectable lifetime for the charge-separated radical ion pair of 3.8 ± 0.2 μs. The lifetime of this radical-ion-pair state is comparable to what has been seen in previously studied nanohybrids (Scheme 3): SWNT grafted with poly(sodium 4-styrenesulfonate) (SWNT-PSS^{n-})/octacationic free-base porphyrin salt (H_2P^{8+}), SWNT/linearly-polymerized poly(methyl methacrylate) carrying free-base porphyrin (H_2P-polymer), and SWNT grafted with 1-(trimethylammonium acetyl)pyrene (SWNT/pyrene$^+$)/octaanionic zinc porphyrin salt (ZnP^{8-}).[8e,16v,17b] The radical ion pair decay provides the quantitative recovery of the singlet ground state. Population of the ZnP triplet-excited state is thermodynamically unfeasible, as we will demonstrate below. Notably, in reference experiments with PVP•ZnP and pyridine•ZnP only the long-lived triplet features were detected.

A thermodynamic correlation further supports the experimental observations. For systems composed of SWNT-PVP (the electron acceptor) and ZnP (the electron donor), we find approximate energies of the radical-ion-pair states from the electrochemical reduction of SWNT-PVP (−0.5 V) and

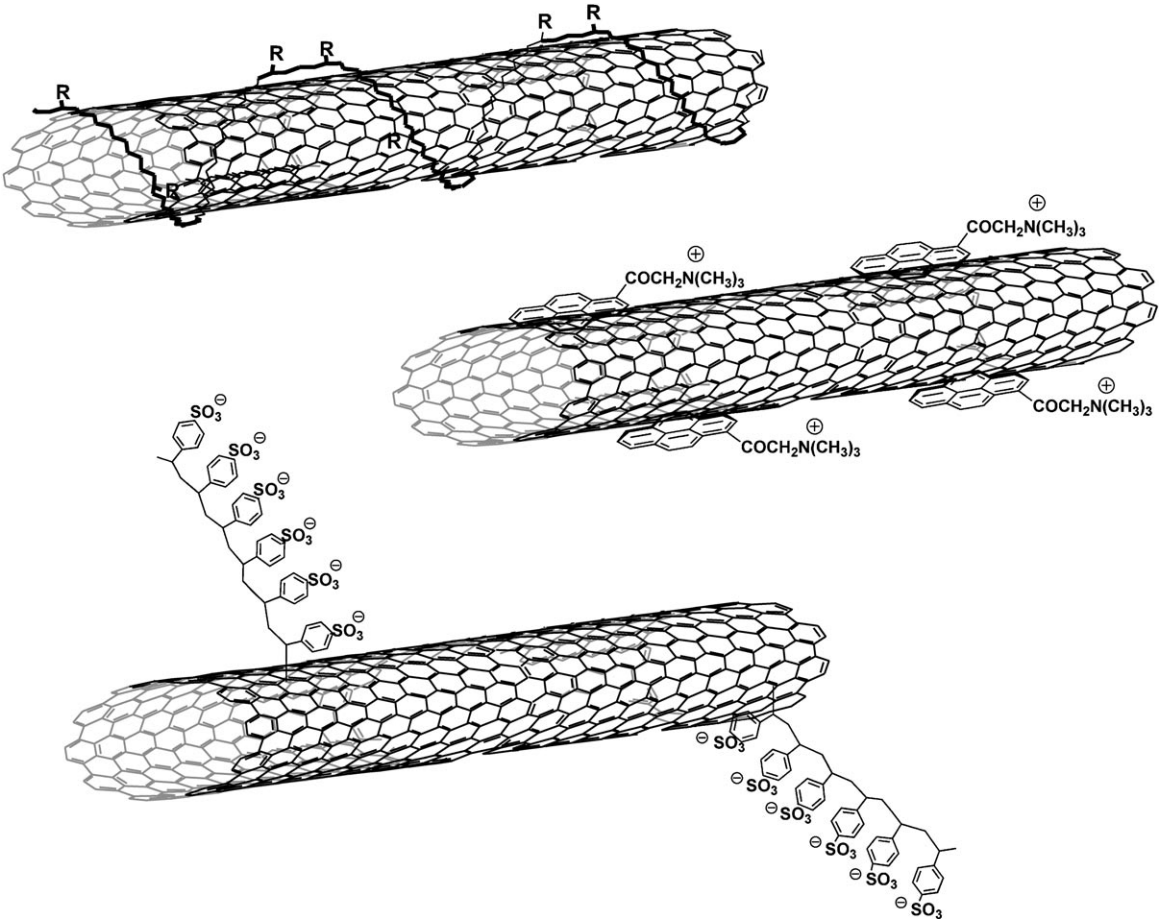

Scheme 3. SWNT-based nanohybrids. Upper part: SWNT/linearly-polymerized poly(methylmethacrylate) carrying free-base porphyrin (H_2P-polymer).[16v] Center part: SWNT grafted with 1-(trimethylammonium acetyl) pyrene (SWNT/pyrene$^+$).[17b] Lower part: SWNT grafted with poly(sodium-4-styrenesulfonate) (SWNT-PSS^{n-}).[8e]

the electrochemical oxidation of ZnP (+0.8 V)[28] to be 1.3 eV. The singlet-excited-state energy, on the other hand, comes from the energy average of the longest wavelength absorption and the shortest wavelength fluorescence. Accordingly, for ZnP the singlet-excited-state energy is 2.1 eV. The triplet-excited-state energy, as directly taken from phosphorescence measurements, is 1.5 eV. We used these values to construct the energy diagram depicted in Figure 10. Implicit are the driving forces for charge separation (evolving from the singlet-excited electron donor) and for charge recombination (decay of the radical-ion-pair state) that are appreciably large with values around 0.8 and 1.3 eV, respectively. Based on the reasonably high polarity of DMF with a dielectric constant of approximately 36 we omit the Coulombic correction term in our correlation.

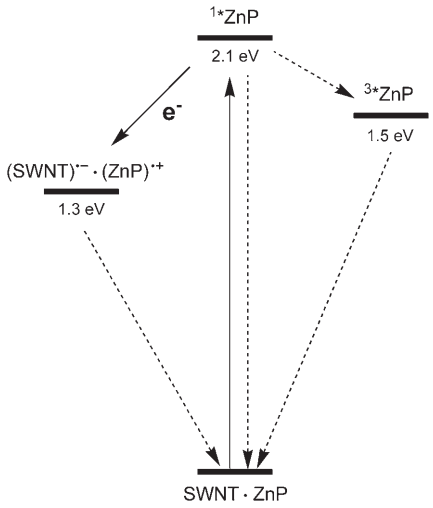

Figure 10. Energy diagram summarizing the states following photoexcitation of SWNT-PVP·ZnP.

Temperature can be used to control the SWNT-PVP·ZnP association. The SWNT-PVP coordination to ZnP is labile and dynamic. Hence, increasing or decreasing the temperature weakens or strengthens the complex, respectively. In this context, fluorescence emerged as a sensitive temperature probe. Temperature increase, for example, led to a notable reactivation of the ZnP fluorescence, while lower temperatures essentially caused deactivation. An illustration is given in Figure 11. The effects were reproducible between temperatures of 10 and 80°C.

Conclusion

Successful coordination was achieved using dispersible single-walled carbon nanotubes grafted with poly(4-vinylpyridine) and ZnP. The novel nanohybrids (SWNT-PVP·ZnP) were characterized in the ground and excited state with specific accent on electron-transfer chemistry.[29] In fact, fluorescence and transient absorption measurements provide kinetic and spectroscopic evidence that support a transfer of charge density. A consequence of strong donor–acceptor coupling is the rapid formation of microsecond-lived radical-ion-pair states.

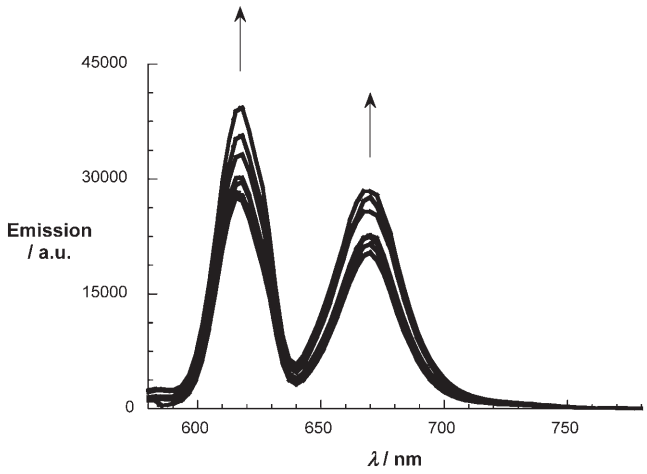

Figure 11. Fluorescence spectra of SWNT-PVP·ZnP in DMF at variable temperatures between 15 and 75°C in increments of 10°C. The excitation wavelength is the isosbestic point at 429 nm. Arrows indicate the fluorescence reactivation with increasing temperature.

Experimental Section

Nanosecond laser flash photolysis experiments were performed with laser pulses from a Quanta-Ray CDR Nd:YAG system (532 nm, 6 ns pulsewidth) in a front-face excitation geometry. The photomultiplier output was digitized with a Tektronix 7912 AD programmable digitizer. Fluorescence lifetimes were measured with a Laser Strobe Fluorescence Lifetime Spectrometer (Photon Technology International) with 337 nm laser pulses from a nitrogen laser fiber-coupled to a lens-based T-formal sample compartment equipped with a stroboscopic detector. Details of the laser strobe systems are described on the manufacture's website, http://www.pti-nj.com. Emission spectra were recorded with a SLM 8100 spectrofluorometer. The experiments were performed at room temperature. A 570 nm long-pass filter in the emission path was used in order to eliminate the interference from the solvent and stray light for recording the fullerene fluorescence. Each spectrum was an average of at least five individual scans and was corrected by using the correction function supplied by the manufacturer, by subtraction of the photomultiplier dark counts signal.

The electrochemical experiments were carried out according to methods and procedures described in reference [8c]. The one-compartment electrochemical cell was airtight with high-vacuum glass stopcocks fitted with either Teflon or Viton O-rings in order to prevent contamination by grease. The connections to the high-vacuum line and to the Schlenk flask containing the solvent were made by using spherical joints also fitted with O-rings. The pressure in the electrochemical cell prior to performing the trap-to-trap distillation of the solvent, ranged typically from 1.0–2.0x10^{-5} mbar. The working electrode consisted of a platinum-disc microelectrode (r = 125 μm) sealed in glass. The counter electrode consisted of a platinum spiral and the quasi-reference electrode was a silver spiral. Voltammograms were recorded with an AMEL Model 552 potentiostat or a custom-made fast potentiostat controlled by either an AMEL Model 568 function generator or an ELCHEMA Model FG-206 F. Data acquisition was performed by a Nicolet Model 3091 digital oscilloscope

interfaced to a PC. Temperature was controlled within 0.1 °C with a Lauda RLS thermostat.

Acknowledgements

Part of this work was supported by the Office of Basic Energy Sciences of the U.S. Department of Energy (NDRL-4649 from the Notre Dame Radiation Laboratory), U.S. National Science Foundation (grant EPS-0132354), the Deutsche Forschungsgemeinschaft SFB 583), EU (RTN network "WONDERFULL"), MIUR (cofin prot. 2004035502 and 2004035330), the University of Bologna, and the Fonds der Chemischen Industrie.

[1] a) *Introduction to Nanotechnology*, (Eds.: C. P. Poole, F. J. Owens), Wiley-VCH, Weinheim, **2003**; b) *Nanophysics and Nanotechnology: An Introduction to Modern Concepts in Nanoscience* (Ed.: E. L. Wolf), Wiley, New York, **2004**; c) *Nanoarchitectures and Nanostructured Materials*, (Eds.: Y. Champion, H.-J. Fecht), Wiley-VCH, Weinheim, **2004**.

[2] a) P. Harris, *Carbon Nanotubes and Related Structures: New Materials for the Twenty-First Century*, Cambridge University Press, Cambridge, **2001**; b) *Carbon Nanotubes: Synthesis, Structure, Properties, and Applications* (Eds.: M. S. Dresselhaus, G. Dresselhaus, P. Avouris), P. Springer, Berlin, **2001**; c) S. Reich, C. Thomsen, J. Maultzsch, *Carbon Nanotubes: Basic Concepts and Physical Properties*, Wiley-VCH, Weinheim, **2004**; d) S. Roth, D. Caroll, *One-Dimensional Metals*, Wiley-VCH, Weinheim, **2004**.

[3] Special issue on Carbon Nanotubes, *Acc. Chem. Res.* **2002**, *35*, 997.

[4] Recent reviews: a) P. M. Ajayan, *Chem. Rev.* **1999**, *99*, 1787; b) A. Hirsch, *Angew. Chem.* **2002**, *114*, 1933; *Angew. Chem. Int. Ed.* **2002**, *41*, 1853; c) J. L Bahr, J. M. Tour, *J. Mater. Chem.* **2002**, *12*, 1952; d) S. Niyogi, M. A. Hamon, H. Hu, B. Zhao, P. Bhomwik, R. Sen, M. E. Itkis, R. C. Haddon, *Acc. Chem. Res.* **2002**, *35*, 1105; e) Y.-P. Sun, K. Fu, Y. Lin, W. Huang, *Acc. Chem. Res.* **2002**, *35*, 1096; f) S. Banerjee, M. G. C. Kahn, S. S. Wang, *Chem. Eur. J.* **2003**, *9*, 1898; g) D. Tasis, N. Tagmatarchis, V. Georgakilas, M. Prato, *Chem. Eur. J.* **2003**, *9*, 4000; h) C. A. Dyke, J. M. Tour, *Chem. Eur. J.* **2004**, *10*, 812; i) N. Tagmatarchis, M. Prato, *J. Mater. Chem.* **2004**, *14*, 437; j) C. A. Dyke, J. M. Tour, *J. Phys. Chem. A* **2004**, *108*, 11151.

[5] a) S. J. Tans, M. H. Devoret, H. Dai, A. Thess, R. E. Smalley, L. J. Geerligs, C. Dekker, *Nature* **1997**, *386*, 474; b) S. J. Tans, A. R. M. Verschnesen, C. Dekker, *Nature* **1998**, *393*, 49; c) J. Kong, N. R. Franklin, C. W. Zhou, M. G. Chapline, S. Peng, K. J. Cho, H. J. Dai, *Science* **2000**, *287*, 622; d) A. Goldoni, R. Larciprete, L. Petaccia, S. Lizzit, *J. Am. Chem. Soc.* **2003**, *125*, 11329.

[6] a) R. H. Baughman, C. X. Cui, A. A. Zakhidov, Z. Iqbal, J. N. Barisci, G. M. Spinks, G. G. Wallace, A. Mazzoldi, D. De Rossi, A. G. Rinzler, O. Jaschinski, S. Roth, M. Kertesz, *Science* **1999**, *284*, 1340; b) A. A. Mamedov, N. A. Kotov, M. Prato, D. M. Guldi, J. P. Wicksted, A. Hirsch, *Nat. Mater.* **2002**, *1*, 190; c) A. B. Dalton, S. Collins, E. Munoz, J. M. Razal, V. H. Ebron, J. P. Ferraris, J. N. Coleman, B. G. Kim, R. H. Baughman, *Nature* **2003**, *423*, 703.

[7] a) D. C. Sorescu, K. D. Jordan, P. Avouris, *J. Phys. Chem. B* **2001**, *105*, 11227; b) A. Javey, J. Guo, Q. Wang, M. Lundstrom, H. J. Dai, *Nature* **2003**, *424*, 654.

[8] a) V. Georgakilas, K. Kordatos, M. Prato, D. M. Guldi, M. Holzinger, A. Hirsch, *J. Am. Chem. Soc.* **2002**, *124*, 760; b) H. Murakami, T. Nomura, N. Nakashima, *Chem. Phys. Lett.* **2003**, *378*, 481; c) D. M. Guldi, M. Marcaccio, D. Paolucci, F. Paolucci, N. Tagmatarchis, D. Tasis, E. Vazquez, M. Prato, *Angew. Chem.* **2003**, *115*, 4338; *Angew. Chem. Int. Ed.* **2003**, *42*, 4206; d) H. Li, B. Zhou, L. Gu, W. Wang, K. A. Shiral Ferando, S. Kumar, J. F. Allard, Y.-P. Sun, *J. Am. Chem. Soc.* **2004**, *126*, 1014; e) D. M. Guldi, G. M. A. Rahman, J. Ramey, M. Marcaccio, D. Paolucci, F. Paolucci, S. Qin, W. T. Ford, D. Balbinot, N. Jux, N. Tagmatarchis, M. Prato, *Chem. Commun.* **2004**, 2034.

[9] a) L. W. Qu, R. B. Martin, W. J. Huang, K. F. Fu, D. Zweifel, Y. Lin, Y.-P. Sun, C. E. Bunker, B. A. Harruff, J. R. Gord, L. F. Allard, *J. Chem. Phys.* **2002**, *117*, 8089; b) H. Murakami, T. Nomura, N. Nakashima, *Chem. Phys. Lett.* **2003**, *378*, 481; c) M. Alvaro, P. Atienzar, P. de la Cruz, J. L. Delgado, H. Garcia, F. Langa, *J. Phys. Chem. B* **2004**, *108*, 12691; d) R. B. Martin, L. W. Qu, Y. Lin, B. A. Harruff, C. E. Bunker, J. R. Gord, L. F. Allard, Y.-P. Sun, *J. Phys. Chem. B* **2004**, *108*, 11447; e) M. Alvaro, P. Atienzar, J. L. Bourdelande, H. Garcia, *Chem. Phys. Lett.* **2004**, *384*, 119.

[10] a) E. Kymakis, G. A. J. Amaratunga, *Appl. Phys. Lett.* **2002**, *80*, 112; b) E. Kymakis, G. A. J. Amaratunga, *Sol. Energy Mater. Sol. Cells* **2003**, *80*, 465; c) E. Kymakis, I. Alexandrou, *J. Appl. Phys.* **2003**, *93*, 1764; d) C. Yang, M. Wohlgenannt, Z. V. Vardeny, W. J. Blau, A. B. Dalton, R. Baughman, A. A. Zakhidov, *Physica B+C* **2003**, *338*, 366; e) S. Barazzouk, S. Hotchandani, V. Vinodgopal, P. V. Kamat, *J. Phys. Chem. A* **2004**, *108*, 17015; f) L. Sheeney-Hai-Ichia, B. Basnar, I. Willner, *Angew. Chem.* **2005**, *117*, 80; *Angew. Chem. Int. Ed.* **2005**, *44*, 78.

[11] a) R. J. Chen, Y. Zhang, D. Wang, H. Dai, *J. Am. Chem. Soc.* **2001**, *123*, 3838; b) M. Shim, N. W. S. Kim, R. J. Chen, Y. Li, H. Dai, *Nano Lett.* **2002**, *2*, 285; c) D. Pantarotto, C. D. Partidos, R. Graff, J. Hoebeke, J.-P. Briand, M. Prato, A. Bianco, *J. Am. Chem. Soc.* **2003**, *125*, 6160; d) S. G. Chou, H. B. Ribeiro, E. B. Barros, A. P. Santos, D. Nezich, G. G. Samsonidze, C. Fantini, M. A. Pimenta, A. Jorio, F. Plentz, M. S. Dresselhaus, G. Dresselhaus, R. Saito, M. Zheng, G. B. Onoa, S. D. Semke, A. K. Swan, M. S. Unlu, B. B. Goldberg, *Chem. Phys. Lett.* **2004**, *397*, 296; e) I. C. Yeh, G. Hummer, *Proc. Natl. Acad. Sci. USA* **2004**, *101*, 12177; f) Y. Lin, S. Taylor, H. P. Li, K. A. S. Fernando, L. W. Qu, W. Wang, L. R. Gu, B. Zhou, Y.-P. Sun, *J. Mater. Chem.* **2004**, *14*, 527; g) M. Zheng, A. Jagota, M. S. Strano, A. P. Santos, P. Barone, S. G. Chou, B. A. Diner, M. S. Dresselhaus, R. S. McLean, G. B. Onoa, G. G. Samsonidze, E. D. Semke, M. Usrey, D. J. Walls, *Science* **2004**, *302*, 1545; h) D. Pantarotto, R. Singh, D. McCarthy, M. Erhardt, J.-P. Briand, M. Prato, K. Kostarelos, A. Bianco, *Angew. Chem.* **2004**, *116*, 5354; *Angew. Chem. Int. Ed.* **2004**, *43*, 5242; i) R. Singh, D. Pantarotto, D. McCarthy, O. Chaloin, J. Hoebeke, C. D. Partidos, J. P. Briand, M. Prato, A. Bianco, K. Kostarelos, *J. Am. Chem. Soc.* **2005**, *127*, 4388.

[12] see for example: M. Holzinger, A. Hirsch, P. Bernier, G. S. Duesberg, M. Burghard, *Appl. Phys. A* **2000**, *70*, 599.

[13] a) A. C. Dillon, T. Gennett, K. M. Jones, J. L. Alleman, P. A. Parilla, M. J. Heben, *Adv. Mater.* **1999**, *11*, 1354; b) W. Chiang, B. E. Brinson, R. E. Smalley, J. L. Margrave, R. H. Hauge, *J. Phys. Chem. B* **2001**, *105*, 1157; c) M. S. Strano, C. A. Dyke, M. L. Usrey, P. W. Barone, M. J. Allen, H. Shan, C. Kittrell, R. H. Hauge, J. M. Tour, R. E. Smalley, *Science* **2003**, *301*, 1519; d) E. Zurek, J. Autschbach, *J. Am. Chem. Soc.* **2004**, *126*, 13079.

[14] a) V. Georgakilas, D. Voulgaris, E. Vazquez, M. Prato, D. M. Guldi, A. Kukovecz, H. Kuzmany, *J. Am. Chem. Soc.* **2002**, *124*, 14318; b) D. M. Guldi, M. Holzinger, A. Hirsch, V. Georgakilas, M. Prato, *Chem. Commun.* **2003**, 1130.

[15] a) L. Chico, V. H. Crespi, L. X. Benedict, S. G. Louie, M. L. Cohen, *Phys. Rev. Lett.* **1996**, *76*, 971; b) D. L. Carroll, P. Redlich, P. M. Ajayan, J. C. Charlier, X. Blasé, A. DeVita, R. Car, *Phys. Rev. Lett.* **1997**, *78*, 2811; c) A. A. Maarouf, C. L. Kane, E. J. Mele, *Phys. Rev. B* **2000**, *61*, 11156; d) S. G. Lemay, J. W. Janssen, M. van den Hout, M. Mooij, M. J. Bronikowski, P. A. Willis, R. E. Smalley, L. P. Kouwenhoven, C. Dekker, *Nature* **2001**, *412*, 617; e) P. Avouris, *Chem. Phys.* **2002**, *281*, 429; f) M. Brandbyge, J. L. Mozos, P. Ordejon, J. Taylor, K. Stokbro, *Phys. Rev. B* **2002**, *65*, 165401.

[16] a) S. A. Curran, P. M. Ajayan, W. J. Blau, D. L. Carroll, J. N. Coleman, A. B. Dalton, A. P. Davey, A. Drury, B. McCarthy, S. Maier, A. Strevens, *Adv. Mater.* **1998**, *10*, 1091; b) M. A. Hamon, J. Chen, H. Hu, Y. Chen, M. E. Itkis, A. M. Rao, R. C. Eklund, R. C. Haddon, *Adv. Mater.* **1999**, *11*, 834; c) B. Z. Tang, H. Xu, *Macromolecules* **1999**, *32*, 2569; d) J. N. Coleman, A. B. Dalton, S. Curran, A. Rubio, A. P. Davey, A. Drury, B. McCarthy, B. Lahr, P. M. Ajayan, S. Roth, R. C. Barklie, W. J. Blau, *Adv. Mater.* **2000**, *12*, 213; e) A. B. Dalton, C. Stephan, J. N. Coleman, B. McCarthy, P. M. Ajayan, S.

Lefrant, P. Bernier, W. J. Blau, *J. Phys. Chem.* **2000**, *104*, 10012; f) C. Stephan, T. P. Nguyen, M. Lamy de la Chapelle, S. Lefrant, C. Journet, P. Bernier, *Synth. Met.* **2000**, *108*, 139; g) A. Star, J. F. Stoddart, D. Steuerman, M. Dile, A. Boukai, E. W. Wong, X. Yang, S. W. Cheng, H. Choi, J. R. Heath, *Angew. Chem.* **2001**, *113*, 1771; *Angew. Chem. Int. Ed.* **2001**, *40*, 1721; h) M. Yudasaka, M. Zhang, C. Jabs, S. Iijima, *Appl. Phys. A* **2001**, *71*, 449; i) J. Chen, H. Y. Liu, W. A. Weimer, M. D. Halls, D. H. Waldeck, G. C. Walker, *J. Am. Chem. Soc.* **2002**, *124*, 9034; j) A. Star, D. W. Steuerman, J. R. Heath, J. F. Stoddart, *Angew. Chem.* **2002**, *114*, 2618; *Angew. Chem. Int. Ed.* **2002**, *41*, 2508; k) D. W. Steuerman, A. Star, R. Narizzano, H. Choi, R. S. Ries, C. Nicolini, J. F. Stoddart, J. R. Heath, *J. Phys. Chem. B* **2002**, *106*, 3124; l) A. Star, J. F. Stoddart, *Macromolecules* **2002**, *35*, 7516; m) A. Star, Y. Liu, K. Grant, L. Ridvan, J. F. Stoddart, D. W. Steuerman, M. R. Diehl, A. Boukai, J. R. Heath, *Macromolecules* **2003**, *36*, 553; n) G. R. Dieckmann, A. B. Dalton, P. A. Johnson, J. Razal, J. Chen, G. M. Giordano, E. Munzo, I. H. Musselman, R. H. Baughman, R. K. Draper, *J. Am. Chem. Soc.* **2003**, *125*, 1770; o) S. Wang, E. S. Humphreys, S.-Y. Chung, D. E. Delduco, S. R. Lustig, H. Wang, K. N. Parker, N. W. Rizzo, S. Subramoney, Y.-M. Chiang, A. Jagota, *Nat. Mater.* **2003**, *2*, 196; p) M. Zheng, A. Jagota, E. D. Semke, B. A. Diner, R. S. McLean, S. R. Lustig, R. E. Richardson, N. G. Tassi, *Nat. Mater.* **2003**, *2*, 338; q) M. Zheng, A. Jagota, M. S. Strano, P. Barone, S. G. Chou, B. A. Diner, M. S. Dresselhaus, R. S. McLean, G. B. Onoa, G. G. Samsonidze, E. D. Semke, M. Usrey, D. J. Wells, *Science* **2003**, *302*, 1545; r) M. Numata, M. Asai, K. Kaneko, T. Hasegawa, N. Fujita, Y. Kitada, K. Sakurai, S. Shinkai, *Chem. Lett.* **2004**, *33*, 232; s) V. Zorbas, A. Ortiz-Acevedo, A. B. Dalton, M. M. Yoshida, G. R. Dieckmann, R. K. Draper, R. H. Baughman, M. Jose-Yacaman, I. H. Musselman, *J. Am. Chem. Soc.* **2004**, *126*, 7222; t) V. A. Sinani, M. K. Gheith, A. A. Yaroslavov, A. A. Rakhnyanskaya, K. Sun, A. A. Mamedov, J. P. Wicksted, N. A. Kotov, *J. Am. Chem. Soc.* **2005**, *127*, 3463; u) N. R. Raravikar, L. S. Schadler, A. Vijayaraghavan, Y. Zhao, B. Wei, P. M. Ajayan, *Chem. Mater.* **2005**, *17*, 974; v) D. M. Guldi, H. Taieb, G. M. A. Rahman, N. Tagmatarchis, M. Prato, *Adv. Mater.* **2005**, *17*, 871.

[17] a) N. Nakashima, Y. Tomonari, H. Murakami, *Chem. Lett.* **2002**, 638; b) D. M. Guldi, G. M. A. Rahman, N. Tagmatarchis, M. Prato, *Angew. Chem.* **2004**, *116*, 5642; *Angew. Chem. Int. Ed.* **2004**, *43*, 5526; c) A. B. Artyukhin, O. Bakajin, P. Stroeve, A. Noy, *Langmuir* **2004**, *20*, 1442; d) L. S. Fifield, L. R. Dalton, R. S. Addleman, R. A. Galhotra, M. H. Engelhard, G. E. Fryxell, C. L. Aardahl, *J. Phys. Chem. B* **2004**, *108*, 8737; e) J. Zhu, M. Yudasaka, M. F. Zhang, S. Iijima, *J. Phys. Chem. B* **2004**, *108*, 11317; f) D. M. Guldi, G. M. A. Rahman, N. Jux, D. Balbinot, N. Tagmatarchis, M. Prato, *Chem. Commun.* **2005**, 2038; g) G. M. A. Rahman, D. M. Guldi, E. Zambon, L. Pasquato, N. Tagmatarchis, M. Prato, *Small* **2005**, *1*, 527.

[18] D. M. Guldi, G. M. A. Rahman, M. Prato, N. Jux, S. Qin, W. Ford, *Angew. Chem.* **2005**, *117*, 2051; *Angew. Chem. Int. Ed.* **2005**, *44*, 2015.

[19] S. Qin, D. Qin, W. T. Ford, J. E. Herrera, D. E. Resasco, *Macromolecules* **2004**, *37*, 9963.

[20] The strong absorption of PVP leads to a saturation of the absorption spectrum in the UV range.

[21] M. S. Strano, C. A. Dyke, M. L. Usrey, P. W. Barone, M. J. Allen, H. Shan, C. Kittrell, R. H. Hauge, J. M. Tour, R. E. Smalley, *Science* **2003**, *301*, 1519.

[22] a) F. D′Souza, G. R. Deviprasad, M. S. Rahman, J.-P. Choi, *Inorg. Chem.* **1999**, *38*, 2157; b) N. Armaroli, F. Diederich, L. Echegoyen, T. Habicher, L. Flamigni, G. Marconi, J.-F. Nierengarten, *New J. Chem.* **1999**, *23*, 77; c) D. M. Guldi, C. Luo, T. Da Ros, M. Prato, E. Dietel, A. Hirsch, *Chem. Commun.* **2000**, 375; d) F. D′Souza, G. R. Deviprasad, M. E. El-Khouly, M. Fujitsuka, O. Ito, *J. Am. Chem. Soc.* **2001**, *123*, 5277; e) D. M. Guldi, C. Luo, A. Swartz, M. Scheloske, A. Hirsch, *Chem. Commun.* **2001**, 1066; f) T. Da Ros, M. Prato, D. M. Guldi, M. Ruzzi, L. Pasimeni, *Chem. Eur. J.* **2001**, *7*, 816.

[23] a) L. G. Shaidarova, A. V. Gedmina, I. A. Cheinokova, G. K. Budnikov, *J. Anal. Chem.* **2003**, *58*, 886; b) L. G. Shaidarova, A. V. Gedmina, G. K. Budnikov, *J. Anal. Chem.* **2003**, *58*, 171.

[24] In this light we suspended successfully SWNT in DMF solutions with the help of ZnP and H_2P and noted fluorescence quenching.

[25] J. Rodriguez, C. Kirmaier, D. Holten, *J. Am. Chem. Soc.* **1989**, *111*, 6500.

[26] In fact, SWNT-PVP competes with the absorption of photons at the 532 nm excitation wavelength.

[27] See for experimental conditions: D. M. Guldi, P. Neta, P. Hambright, *J. Chem. Soc. Faraday Trans.* **1992**, *88*, 2013, and references therein.

[28] H. Imahori, K. Tamaki, D. M. Guldi, C. Luo, M. Fujitsuka, O. Ito, Y. Sakata, S. Fukuzumi, *J. Am. Chem. Soc.* **2001**, *123*, 2607.

[29] Intermolecular reactions seem to play no major role in the case of full complexation.

Received: August 1, 2005
Published online: December 21, 2005

